



Universiteit  
Leiden  
The Netherlands

## **The activation mechanisms of G protein-coupled receptors : the case of the adenosine A2B and HCA2/3 receptors**

Liu, R.

### **Citation**

Liu, R. (2016, December 8). *The activation mechanisms of G protein-coupled receptors : the case of the adenosine A2B and HCA2/3 receptors*. Retrieved from <https://hdl.handle.net/1887/44797>

Version: Not Applicable (or Unknown)

License: [Licence agreement concerning inclusion of doctoral thesis in the Institutional Repository of the University of Leiden](#)

Downloaded from: <https://hdl.handle.net/1887/44797>

**Note:** To cite this publication please use the final published version (if applicable).

Cover Page



Universiteit Leiden



The handle <http://hdl.handle.net/1887/44797> holds various files of this Leiden University dissertation

**Author:** Rongfang Liu

**Title:** The activation mechanisms of G protein-coupled receptors : the case of the adenosine A2B and HCA2/3 receptors

**Issue Date:** 2016-12-08

## Chapter 3

# **A yeast screening method to decipher the interaction between the adenosine A<sub>2B</sub> receptor and the C-terminus of different G protein $\alpha$ -subunits**

This chapter is based upon:

Rongfang Liu, Nick J. A. Groenewoud, Miriam C. Peeters, Eelke B. Lenselink, Ad P. IJzerman

*Purinergic Signalling* **2014** 10: 441-453



## Abstract

The expression of human G protein-coupled receptors (GPCRs) in *Saccharomyces cerevisiae* containing chimeric yeast/mammalian  $G_{\alpha}$  subunits provides a useful tool for the study of GPCR activation. In this study, we used a one-GPCR-one-G protein yeast screening method in combination with molecular modeling and mutagenesis studies to decipher the interaction between GPCRs and the C-terminus of different  $\alpha$ -subunits of G proteins. We chose the human adenosine  $A_{2B}$  receptor ( $hA_{2B}R$ ) as a paradigm, a typical class A GPCR that shows promiscuous behavior in G protein coupling in this yeast system. The wild-type  $hA_{2B}R$  and five mutant receptors were expressed in 8 yeast strains with different humanized G proteins, covering the four major classes:  $G_{\alpha i}$ ,  $G_{\alpha s}$ ,  $G_{\alpha q}$  and  $G_{\alpha 12}$ . Our experiments showed that a tyrosine residue (Y) at the C-terminus of the  $G_{\alpha}$  subunit plays an important role in controlling the activation of GPCRs. Receptor residues R103<sup>3,50</sup> and I107<sup>3,54</sup> are vital too in G protein-coupling and the activation of the  $hA_{2B}R$ , whereas L213<sup>L3</sup> is more important in G protein inactivation. Substitution of S235<sup>6,36</sup> to alanine provided the most divergent G protein coupling profile. Finally, L236<sup>6,37</sup> substitution decreased receptor activation in all G protein pathways, although to a different extent. In conclusion, our findings shed light on the selectivity of receptor/G protein coupling, which may help in further understanding GPCR signaling.

## Introduction

G protein-coupled receptors (GPCRs), also known as seven-transmembrane receptors (7TMRs), are a major class of targets for many of today's medicines, to combat ailments such as inflammation, cardiac malfunction, asthma and cancer. Ligands interact with these transmembrane proteins in many different ways, intervening with or mimicking their activation process, which is mediated mostly by a heterotrimeric G protein, composed of  $\alpha$ ,  $\beta$  and  $\gamma$  subunits<sup>[1, 2]</sup>. However, the exact mechanism of GPCR activation at the molecular level is still largely unknown. Here, we used the hA<sub>2B</sub>R, a typical class A GPCR, as a paradigm to decipher the interaction between receptors and their G proteins.

The adenosine receptors include four subtypes: A<sub>1</sub>R, A<sub>2A</sub>R, A<sub>2B</sub>R and A<sub>3</sub>R, which have attracted much attention as therapeutic targets in recent years. All the adenosine receptors are ubiquitously expressed in the human body<sup>[3]</sup> and can target different intracellular signaling pathways by responding to the same endogenous ligand adenosine. The A<sub>2B</sub>R has the lowest affinity for adenosine<sup>[4]</sup> and has been less investigated than other adenosine receptors. Several studies have shown that blocking A<sub>2B</sub>R signaling reduces experimental autoimmune encephalomyelitis<sup>[5]</sup> and inhibits growth of prostate cancer cells<sup>[6]</sup>, breast tumors<sup>[7]</sup> and bladder tumors<sup>[8, 9]</sup>. On the other hand, stimulation of A<sub>2B</sub>R protects against trauma-hemorrhagic shock-induced lung injury<sup>[10]</sup>, CHX-induced apoptosis<sup>[6]</sup> and also vascular injury<sup>[11]</sup>.

Yeast can provide a powerful platform for studying GPCRs and their G protein coupling and selectivity. *Saccharomyces cerevisiae* (*S. cerevisiae*) strains, each expressing a specific human G <sub>$\alpha$</sub> /yeast Gpa1 protein chimera, have been used to express heterologous GPCRs, for instance in high-throughput screening assays for drug discovery<sup>[12]</sup>, to perform random mutagenesis screening<sup>[13, 14]</sup>, and to assess the preference of G <sub>$\alpha$</sub>  pathways<sup>[15]</sup> and functional selectivity of agonists and antagonists<sup>[16-18]</sup>. Several lines of evidence indicate that the C-terminal five amino acid residues of a G protein are sufficient for coupling with many human receptors, including the hA<sub>2B</sub>R<sup>[19]</sup>. One of the advantages of the yeast system used is that while these five amino acids of many human G protein  $\alpha$ -subunits were

'transplanted' to replace these residues on the yeast's endogenous G protein, Gpa1p (see also Table 1), all other aspects of the system remain the same and intact<sup>[20, 21]</sup>.

In the present study, we used this one-GPCR-one-G protein yeast screening method in combination with molecular modeling and mutagenesis studies. Our goal was to provide more information about the mechanism of activation of the hA<sub>2B</sub>R and the role the binding pocket for the G<sub>α</sub> protein's C-terminus plays in that process. Our findings provide further evidence for the A<sub>2B</sub> receptor's G protein preferences, which in itself may be useful for designing and screening selective agonists and antagonists for this receptor. At the same time, our findings have a broader relevance as they reflect on the GPCR-G protein interface.

**Table 1.** The genotypes of the yeast strains used for transformations<sup>[20, 21, 49]</sup>.

| Strain                    | Genotype  | The five C-terminal residues of G <sub>α</sub> |
|---------------------------|---|--|
| MMY11                     | <b>MATa</b> <i>his3 ade2 leu2 trp1 ura3 can1 fus1::FUS1-HIS3 FUS1-lacZ::LEU2 farΔ::ura3Δgpa1Δ::ADE2Δsst2Δ::ura3Δste2Δ::G418<sup>R</sup></i> |  |
| MMY12 (G <sub>αWT</sub> ) | MMY11TRP1:: <i>GPA1</i>   | KIGII <sup>COOH</sup>                          |
| MMY23 (G <sub>αi1</sub> ) | MMY11TRP1:: <i>Gpa1/G<sub>αi1(5)</sub></i>  | DCGLF <sup>COOH</sup>                          |
| MMY24 (G <sub>αi3</sub> ) | MMY11TRP1:: <i>Gpa1/G<sub>αi3(5)</sub></i>  | ECGLY <sup>COOH</sup>                          |
| MMY28 (G <sub>αs</sub> )  | MMY11TRP1:: <i>Gpa1/G<sub>αs(5)</sub></i>   | QYELL <sup>COOH</sup>                          |
| MMY14 (G <sub>αq</sub> )  | MMY11TRP1:: <i>Gpa1/G<sub>αq(5)</sub></i>   | EYNLV <sup>COOH</sup>                          |
| MMY21 (G <sub>α14</sub> ) | MMY11TRP1:: <i>Gpa1/G<sub>α14(5)</sub></i>  | EFNLV <sup>COOH</sup>                          |
| MMY19 (G <sub>α12</sub> ) | MMY11TRP1:: <i>Gpa1/G<sub>α12(5)</sub></i>  | DIMLQ <sup>COOH</sup>                          |
| MMY20 (G <sub>α13</sub> ) | MMY11TRP1:: <i>Gpa1/G<sub>α13(5)</sub></i>  | QLMLQ <sup>COOH</sup>                          |

## Materials and methods

### hA<sub>2B</sub> Receptor/G protein homology modeling

A homology model was created using Molsoft's ICM Homology tool (Version 3.7-2)<sup>[22]</sup>. The  $\beta_2$  adrenergic receptor ( $\beta_2$ AR) in complex with the G<sub>s</sub> protein<sup>[23]</sup> (PDB: 3SN6) was chosen as template since it was the closest (and currently only) homolog of the hA<sub>2B</sub>R containing the G<sub>as</sub> protein, with 30% sequence identity and 48% sequence similarity using a pair-wise sequence alignment method (EMBOSS\_matcher; [http://www.ebi.ac.uk/Tools/psa/emboss\\_matcher/](http://www.ebi.ac.uk/Tools/psa/emboss_matcher/)). The hA<sub>2B</sub>R sequence (uniprot: P29275) was modeled onto 3SN6 and residues were selected to be individually mutated to alanine based on the following two criteria: 1) within 5 Å distance from the last five amino acids of the G<sub>as</sub> protein (QYELL) and 2) oriented towards the G<sub>as</sub> protein. Final visualizations were created using PyMOL (The PyMOL Molecular Graphics System, Version 1.5.0.4 Schrödinger, LLC)<sup>[24]</sup>.

### Generation of point mutations

The *S. cerevisiae* expression vectors, the pDT-PGK and pDT-PGK\_A<sub>2B</sub> receptor plasmids, were kindly provided by Dr. Simon Dowell from GSK (Stevenage, UK). The DNA primers of the mutants of the A<sub>2B</sub> receptor were designed by the QuikChange® Primer Design Program on the website of Agilent Technologies, and contained a single substitution resulting in a codon change for the desired amino acid substitution. The reverse primer sequence of each mutant was the reverse complement of the forward primer. These primers and their complements were synthesized (Eurogentec, the Netherlands) and then used to generate mutant plasmids according to the QuikChange method from Stratagene. The mutagenic reaction contained 40 ng of the pDT-PGK\_A<sub>2B</sub> construct plasmid as dsDNA template, 10 µM of each primer, 1 µl of dNTP mix, 2.5 µl of 10× reaction buffer and 2.5 U *PfuUltra* HF DNA polymerase. The following thermal cycling parameters were used in the PCR apparatus (T100™ Thermal Cycler, BIO-RAD): 95 °C for 30 s, 55 °C for 1 min, and 68 °C for 10 min. The number of mutagenic PCR cycles was set to 20. Methylated or hemimethylated non-mutated plasmid

DNA was removed by adding 5 U *Dpn* I restriction enzyme for 2 h at 37 °C. The mutated DNA products were transformed into XL-1 Blue supercompetent cells and other details were according to the manual of the QuikChange® II Site-Directed Mutagenesis Kit. Mutant plasmids were isolated from a single clone using a QIAprep midi plasmid purification kit (QIAGEN, the Netherlands). The mutants were confirmed by DNA sequencing (LGTC, Leiden, the Netherlands).

### Transformation in *S. cerevisiae* strains

Each mutant plasmid was transformed according to the Lithium-Acetate procedure<sup>[25]</sup> into a panel of engineered *S. cerevisiae* yeast strains expressing different Gpa1p/G<sub>α</sub> chimeras. The yeast strains were derived from the MMY11 strain and further adapted to communicate with mammalian GPCRs. The difference between these integrated Gpa1p/G<sub>α</sub> chimeras is that the last five amino acids of the endogenous Gpa1p C-terminus have been replaced with the same sequence as that from mammalian G<sub>α</sub> proteins<sup>[20, 21]</sup> (Table 1). To measure the signaling of GPCRs, the pheromone signaling pathway of these strains was coupled via the *FUS1* promoter to *HIS3* (imidazoleglycerol-phosphate dehydratase), an enzyme catalyzing the sixth step in histidine biosynthesis to produce histidine. 3-AT (3-amino-[1, 2, 4]- triazole), a competitive inhibitor of imidazoleglycerol-phosphate dehydratase, was added to the assay to reduce background activity caused by endogenous histidine<sup>[20]</sup>. The degree of receptor activation induced by an agonist of the GPCR was measured by the growth rate of the yeast on histidine-deficient medium.

### Liquid growth assay

To measure the efficiency of GPCR-G protein coupling, concentration-growth curves were generated in a liquid growth assay<sup>[26]</sup>. This assay was carried out in 96-well plates and the growth was determined by measuring the absorption at a wavelength of approx. 600 nm (OD<sub>600</sub>). To set up an assay, cells were grown to saturation selecting for the transformed plasmid, then seeded at low cell density (2×10<sup>4</sup> cells/ml) into assay medium (YNB + adenine + tryptophan + 10mM 3-AT) lacking histidine and dispensed into assay plates containing the adenosine

receptor agonist NECA ( $10^{-9}$  –  $10^{-4}$  M). The 96-well plate was then incubated for 35 h at 30 °C in a Genios plate reader (Tecan, Durham, NC), keeping the cells in suspension by shaking every 10 min at 300 rpm for 1 min. Results were obtained from two independent experiments, performed in duplicate.  $EC_{50}$  values and  $E_{max}$  values of the liquid assay were analyzed using the nonlinear regression package available in Prism 5.0 software (GraphPad Software Inc., San Diego, CA, USA).

### **Whole cell radioligand binding experiments**

Yeast cells from an overnight culture expressing the wild-type or mutated  $hA_{2B}R$  were harvested from rich YAPD medium by centrifuging 2,000 *g* for 5 min. The pellet of cells was washed once with 0.9% NaCl. The cells were centrifuged again using the same speed and diluted in the assay buffer (50 mM Tris-HCl pH7.4 + 1 mM EDTA) to  $OD_{600} = 40$  ( $OD_{600} = 1 \approx 2.5 \times 10^7$  cells/ml). Binding experiments were performed with 1.5 nM of the  $A_{2B}$  receptor selective antagonist [ $^3H$ ]PSB-603, and a final cell concentration of  $25 \times 10^7$  cells/ml in a total volume of 100  $\mu$ l. Nonspecific binding (NSB) was determined by additionally adding NECA at a final concentration of 1 mM. Samples were incubated for 1 h at 25 °C keeping the cells in suspension by shaking vigorously. 1 ml of ice-cold assay buffer was added to samples to terminate incubation and the samples were harvested on a Millipore manifold with GF/B filters pre-incubated in 0.1% polyethylenimine (PEI) at a pressure of 200 mbar, to separate free from receptor-bound radioligand by washing twice with 2 ml buffer (50 mM Tris-HCl pH7.4 + 1 mM EDTA + 0.1% BSA). The filters were transferred into mini-vials and 3.5 ml of PerkinElmer Emulsifier Safe was added, and subsequently incubated for at least 2 h. Filter-bound radioactivity was determined as counts per minute by scintillation spectrometry (Tri-Carb 2900TR; PerkinElmer Life and Analytical Sciences). Results were obtained from at least three independent experiments, performed in duplicate.

### **Preparation of yeast protein extractions and immunoblotting**

Protein extractions were performed with trichloroacetic acid (TCA) according to

the Clontech Yeast Protocols Handbook 2001. Yeast transformants were grown in 2 ml YAPD medium and were harvested in mid-exponential phase ( $1.2 \times 10^8$  cells). The yeast cells were collected and washed with cold water. Subsequently the yeast cells were broken by vigorous vortexing with 20% TCA and glass beads. The broken yeast cells and the glass beads were washed twice with 200  $\mu$ l 5% TCA and centrifuged at 3,000 rpm for 2 minutes. The supernatant was collected and centrifuged again at 6,000 rpm for 2 minutes. The pellets were resuspended with cold SDS/PAGE loading buffer (100 mM EDTA, 1 M Tris, 10% SDS, 0.5% Bromophenol blue) and 1 M Tris was added to neutralize all remaining TCA. The samples were incubated for 30 min at 37 °C and centrifuged again at 2,000 rpm for 10 min.

Each sample of 4  $\mu$ l containing 24  $\mu$ g protein was loaded on 12.5% SDS/PAGE gel and then blotted on Hybond-ECL membranes (GE Healthcare, the Netherlands) using a semi-automated electrophoresis technique (PhastSystem™, Amersham Pharmacia Biotech). The Hybond-ECL membranes were blocked with TBS containing 5% milk powder for 1 h and washed three times with TBST (0.05% Tween-20, TBS pH 7.6). The membranes were incubated with 1:1250 diluted rabbit anti-human A<sub>2B</sub> receptor antibody for 1 h. This antibody was directed against the C-terminal region of the A<sub>2B</sub>R and was kindly provided by Dr. I. Feoktistov (Vanderbilt University, Nashville)<sup>[27]</sup>. After thorough removal of unbound antibody from the membranes by washing three times with TBST, the membranes were incubated with 1:2,500 diluted HRP-conjugated goat anti-rabbit IgG (Jackson ImmunoResearch Laboratories) for 1 h. The membranes were washed twice with TBST and once with TBS. The specific signal of the A<sub>2B</sub> receptor was probed according to the ECL Western blotting analysis system (GE Healthcare, the Netherlands) using enhanced chemiluminescence (ChemiDox XRS, BIO-RAD). The nonspecific band at approx. 45 kDa was used as loading control and the specific hA<sub>2B</sub>R protein bands were at 29 kDa and 48 kDa. The ratio was determined between the density of the specific bands and density of the nonspecific band that was always present on the blots. MMY12 carrying wild-type or mutant receptor was set as 100% and MMY12 carrying the empty vector pDT-PGK without receptor was set as 0%.

## Results

### G protein selectivity of the wild-type hA<sub>2B</sub> receptor

To investigate the activation mechanism of the hA<sub>2B</sub> receptor at the interface of the C terminus of the G protein G<sub>α</sub> subunit, we expressed the yeast plasmid pDT-PGK\_hA<sub>2B</sub>R in a panel of eight yeast *S. cerevisiae* strains with humanized G proteins. Corresponding to the replaced last five C-terminal residues of the mammalian G<sub>α</sub> subunit, they were classified into five families: G<sub>αWT</sub> (MMY12), G<sub>αs</sub> (MMY28), G<sub>αi</sub> (MMY23 and MMY24), G<sub>α12</sub> (MMY19 and MMY20), and G<sub>αq</sub> (MMY14 and MMY21) (Table 1)<sup>[19]</sup>. When the expressed hA<sub>2B</sub> receptor is activated by an agonist, the yeast pheromone signalling pathway is activated through a chimeric yeast/mammalian G protein leading to subsequent transcription of the HIS3 reporter gene and consequently histidine production<sup>[28]</sup>. Subsequent growth of the yeast cells on histidine-deficient medium was determined by measuring the absorption at a wavelength of 595 nm, which reflects the activation of the expressed receptor by the adenosine receptor agonist NECA. Concentration-response curves of NECA on the wild-type receptor in MMY28(G<sub>αs</sub>), MMY24(G<sub>αi3</sub>), MMY12(G<sub>αWT</sub>), MMY19(G<sub>α12</sub>) and MMY14(G<sub>αq</sub>) are shown in Figure 1 and the values of EC<sub>50'</sub> and E<sub>max</sub> of all strains are shown in Table 2.

We found the five humanized different G protein pathways MMY28(G<sub>αs</sub>), MMY24(G<sub>αi3</sub>), MMY21(G<sub>αi4</sub>), MMY23(G<sub>αi1</sub>) and MMY20(G<sub>αi3</sub>) to show varying degrees of enhancement compared to the coupling efficiency of the wild-type hA<sub>2B</sub>R in the wild-type yeast G<sub>α</sub> strain MMY12(G<sub>αWT</sub>). The most efficient yeast strain MMY28(G<sub>αs</sub>) showed a significant 15-fold improvement in coupling efficiency and also MMY24(G<sub>αi3</sub>) showed a significant 6.5-fold enhancement in coupling efficiency. Two strains, MMY14(G<sub>αq</sub>) and MMY19(G<sub>α12</sub>), responded less to NECA, with significantly higher EC<sub>50</sub> values for this agonist. In terms of intrinsic activity (E<sub>max</sub> values) there was little difference between the strains, however. The one exception was in MMY28(G<sub>αs</sub>) with a large degree of constitutive activity (approx. 30% of the maximal response of MMY12 in response to the agonist NECA (10<sup>-4</sup> M). This may be a feature of the MMY28 strain itself since expression of plasmid pDT-PGK (without any receptor) yielded a similar degree

of constitutive activity (data not shown).

### Bioinformatics and Molecular Modeling

To further decipher the interaction between the hA<sub>2B</sub>R and G proteins, we predicted a number of amino acid residues as important for activation of G proteins from hA<sub>2B</sub>R homology modeling. There are more than 75 crystal structures of 18 different class A GPCRs now<sup>[29]</sup>, however, only two receptors, β<sub>2</sub>AR and opsin (Ops), have been cocrystallised with the G<sub>αs</sub> protein<sup>[23]</sup> and an 11 amino acid synthetic peptide of G<sub>αt</sub><sup>[30]</sup>, respectively. The β<sub>2</sub>AR-G<sub>s</sub> crystal structure (PDB: 3SN6) was chosen as template for mapping amino acid residues of hA<sub>2B</sub>R that are involved in G protein activation. The hβ<sub>2</sub>AR shares 30% sequence identity with the hA<sub>2B</sub>R (Fig. 2A), compared to 23% homology with bovine opsin. In many mammalian cells, the hA<sub>2B</sub>R prefers to couple to G<sub>s</sub> next to G<sub>q</sub> proteins<sup>[31]</sup>, another indication of the validity of this particular homology modeling approach. The model predicted 16 amino acids to interact with G<sub>αs</sub> (i.e. with QYELL, the last five amino acid residues of it): D102<sup>3.49</sup>, R103<sup>3.50</sup>, A106<sup>3.53</sup>, I107<sup>3.54</sup>, Y113<sup>3.60</sup>, I205<sup>5.61</sup>, A209<sup>5.65</sup>, Q212<sup>IL3</sup>, L213<sup>IL3</sup>, R215<sup>IL3</sup>, H231<sup>6.32</sup>, A232<sup>6.33</sup>, S235<sup>6.36</sup>, L236<sup>6.37</sup>, R293<sup>8.46</sup>, N294<sup>8.47</sup>.

Arginine (R) 103<sup>3.50</sup>, isoleucine (I) 107<sup>3.54</sup>, leucine (L) 213<sup>IL3</sup>, serine (S) 235<sup>6.36</sup> and leucine (L) 236<sup>6.37</sup> were selected for mutation into alanine as they are both closest to the G<sub>αs</sub> protein and with their side chains oriented towards the G<sub>αs</sub> protein as well (Fig. 2B). These selected five residues are also shown in the snake plot of the hA<sub>2B</sub>R (Fig. 2C). R103<sup>3.50</sup> and I107<sup>3.54</sup> are located on the intracellular side of TM3 and are included in the consensus sequence (I/L)XXDR<sup>3.50</sup>YXX(I/V)<sup>3.54</sup><sup>[32]</sup>. R<sup>3.50</sup> is a part of the most conserved motif in the class A GPCRs: Asp-Arg-Tyr (DRY). The residues on positions 3.50, 3.54 and 6.36 according to Ballesteros-Weinstein numbering<sup>[33]</sup> are also conserved as part of the G protein-binding region in the bovine opsin-G<sub>t</sub> peptide crystal structure<sup>[23, 29, 30]</sup>.

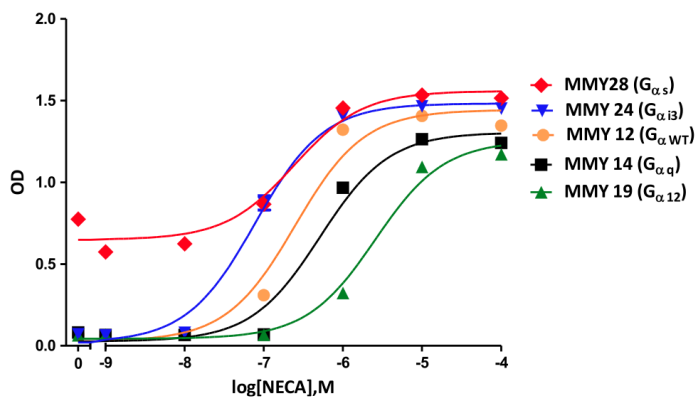


**Fig. 1** Concentration-effect curves from liquid assay experiments are shown of the  $A_{2B}$  wild-type receptor in MMY28 ( $G_{\alpha_s}$ ), MMY24 ( $G_{\alpha_{i3}}$ ), MMY12 ( $G_{\alpha_{WT}}$ ), MMY14 ( $G_{\alpha_q}$ ) and MMY19 ( $G_{\alpha_{12}}$ ) responding to the adenosine receptor agonist NECA. The assay was performed in YNB-ULH medium.

### G protein coupling profiles of five mutant $A_{2B}$ receptors

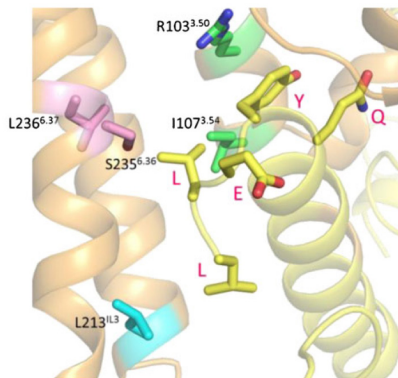
To assess the function of these five residues in G protein activation, we performed a functional yeast liquid assay to determine whether the G protein activation profiles of these mutants had changed or not. NECA concentration-response curves revealed that all five single amino acid changes in the receptor resulted in substantially different humanized G protein coupling profiles of the  $hA_{2B}R$  (Table 2; Fig. 3).

The R103<sup>3.50</sup>A receptor failed to couple to all humanized G protein pathways except for MMY28( $G_{\alpha_s}$ ) with a comparable  $EC_{50}$  value, only 2-fold higher than wild-type receptor (Table 2). Mutant receptor I107<sup>3.54</sup>A only responded with higher than wild-type  $EC_{50}$  values for NECA of 7629 nM to MMY23( $G_{\alpha_{i1}}$ ) with a reduced  $E_{max}$  value of 37%, and 47 nM to MMY28( $G_{\alpha_s}$ ) with a maximal activation level. Other humanized G protein pathways did not respond to NECA anymore (Table 2).

A

|       |     |   |     |
|-------|-----|---|-----|
| A2B   | 11  | VALELVIAALSVAAGNVLVCAVGTANTLQTPNTNYFLVLSAAADVAVGLFA | 60  |
| beta2 | 38  | IVMSLVLVLAIVFGNVLVITAIAKFERLQVTNYFITSLACADLVMLGAV   | 86  |
| A2B   | 61  | IPFAITISLGFCTDF--YGCLFLACFVLVLTQSSIFSLAVADVRYLAIC   | 108 |
| beta2 | 87  | VPFGAAILMKMWTFGNFWCFWTSIDVLCVTASLETLCVIAVDRYFAIT    | 136 |
| A2B   | 109 | VPLRYKSLVTGTRARGVIAVLVWVLAFLGIGLTPF-LGW-NSKDSATNCTE | 156 |
| beta2 | 137 | SPFKYQSLLTKNKARVITLMVWIVSGLISFLPIQMHWYRATHQEAINCYA  | 186 |
| A2B   | 157 | P---WDGTTNESCLVKCLFENVVPMYSMV--YFNFFGCVLPPLLMLVI    | 201 |
| beta2 | 187 | NETCCDFTNQAYAIASSIVSFYVPLVIMVFVYSRVFQEAQRQLQKIDKS   | 236 |
| A2B   | 202 | YIKIFLVACRQLQRTELMDH---SRTTLQREIHAASKLAMIVGIFALCW   | 247 |
| beta2 | 237 | EGRFHVQLNSQVEQDGRGTGHGLRRSSKFLKEHKALKTLGIIMGFTFLCW  | 286 |
| A2B   | 248 | LPVHAVNCVLEFQPAQGNKPKWAMMALLSHANSVVPPIVYAYRNRF      | 297 |
| beta2 | 287 | LPFFIVNIHVHQDNLIRKEVYILLNW---IGYVNSGFNPLIYC-RSPDF   | 332 |
| A2B   | 298 | RYTFHKIL  | 305 |
| beta2 | 333 | RIAFQELL  | 340 |

B



C

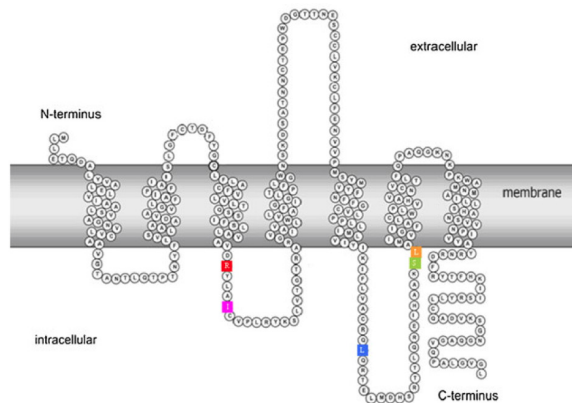


**Fig. 2** (A) Sequence alignment (most similar regions only) between the hA<sub>2B</sub>R (A<sub>2B</sub>; uniprot: P29275) and the hβ<sub>2</sub>AR (beta2; uniprot:P07550). Conserved residues are shown as | between the two sequences. (B) A hA<sub>2B</sub> Receptor/ G<sub>s</sub> protein homology model was generated from the crystal structure of the β<sub>2</sub>AR in contact with the G<sub>as</sub> protein<sup>[23]</sup> (PDB: 3SN6) to predict amino acids interacting with G<sub>as</sub>. The last five C-terminal residues of mammalian G<sub>as</sub> subunit are QYELL<sup>COOH</sup>, shown in red. (C) Snake plot of the hA<sub>2B</sub>R. Five residues (R103<sup>3.50</sup>, I107<sup>3.54</sup>, L213<sup>IL3</sup>, S235<sup>5.36</sup> and L236<sup>6.37</sup>) were selected to be individually mutated to alanine based on the homology model in B).

The L213<sup>IL3</sup>A mutant improved coupling efficiency in all yeast strains compared to the wild-type receptor, but to a different extent. The highest coupling efficiency was found in MMY28(G<sub>as</sub>) and MMY19(G<sub>α12</sub>) with a 10-fold decrease of NECA's EC<sub>50</sub> values compared to the wild-type receptor in the same strain. This mutant receptor was also able to reach maximal activation levels in each yeast strain upon activation by NECA except in MMY14(G<sub>αq</sub>) with a somewhat reduced E<sub>max</sub> value of 76%.

The S235<sup>6.36</sup>A mutant receptor showed the most divergent humanized G protein coupling profile. In MMY12 (G<sub>αWT</sub>) and MMY20(G<sub>α13</sub>), this mutant did not alter activation compared to the wild-type receptor in the same strain. However, it showed the largest increase of activation in MMY28(G<sub>as</sub>) with a one log-unit shift for the full agonist NECA's EC<sub>50</sub>, and a 0.3-fold shift in MMY 23(G<sub>α11</sub>) (Table 2). In contrast, this mutant showed a decrease of activation in MMY24(G<sub>αi3</sub>), MMY14(G<sub>αq</sub>) and MMY21(G<sub>α14</sub>) (up to 3.1-fold in MMY21, Table 2) and a complete loss of activation was observed in MMY19(G<sub>α12</sub>). S235<sup>6.36</sup>A was only able to reach near-maximal activation levels in MMY24(G<sub>αi3</sub>) and MMY28(G<sub>as</sub>) strains. In other strains only a partial NECA response of approx. 80% was observed, except for MMY14(G<sub>αq</sub>) (50%) and MMY19(G<sub>α12</sub>) (no activation) (Table 2).

L236<sup>6.37</sup>A showed a decreased response to NECA in the magnitude of 1.3-fold to 21-fold in all yeast strains compared to the wild-type receptor in the same strain (Table 2). L236<sup>6.37</sup>A reached near-maximal activation levels in most strains except for MMY19 (50%), MMY14 (83%) and MMY20 (85%). Interestingly, L236<sup>6.37</sup>A also induced less constitutive activity in MMY28 than other receptors (wild-type and mutated) in this strain (data not shown).

**Table 2.** EC<sub>50</sub>, fold of EC<sub>50</sub> and E<sub>max</sub> values of wild-type and mutant A<sub>2B</sub> receptors in all examined MMY strains. The fold shift of EC<sub>50</sub> was calculated by dividing the EC<sub>50</sub> of the mutant receptor by the EC<sub>50</sub> of the wild-type receptor of the same strain. %E<sub>max</sub> represents the intrinsic activity of the receptor, where the mean maximal growth level of MMY12 carrying wild-type receptor in response to the agonist NECA (10<sup>-4</sup>M) was set as 100%. Results were mostly obtained from two independent experiments, performed in duplicate (individual values in parentheses).

|                               |                        | EC <sub>50</sub>  | fold EC <sub>50</sub> | % E <sub>max</sub> |
|-------------------------------|------------------------|-------------------|-----------------------|--------------------|
| MMY 12<br>(G <sub>wt</sub> )  | Wild-type              | 393 ± 92          | 1                     | 100 ± 3            |
|                               | R103 <sup>3.50</sup> A | -                 | -                     | 13 (17, 9)         |
|                               | I107 <sup>3.54</sup> A | -                 | -                     | 0 (0, 1)           |
|                               | L213 <sup>IL3</sup> A  | 236 (152, 319)    | 0.6                   | 100 (104, 96)      |
|                               | S235 <sup>6.36</sup> A | 384 (309, 459)    | 1                     | 85 (83, 87)        |
|                               | L236 <sup>6.37</sup> A | 3099 (2503, 3694) | 7.9                   | 102 (109, 96)      |
| MMY 14<br>(G <sub>aq</sub> )  | Wild-type              | 1641 ± 552        | 1                     | 99 ± 3             |
|                               | R103 <sup>3.50</sup> A | -                 | -                     | 1 (1, 1)           |
|                               | I107 <sup>3.54</sup> A | -                 | -                     | (0, 0)             |
|                               | L213 <sup>IL3</sup> A  | 483 (461, 504)    | 0.3                   | 76 (75, 77)        |
|                               | S235 <sup>6.36</sup> A | 3109 (2102, 4115) | 1.9                   | 50 (48, 51)        |
|                               | L236 <sup>6.37</sup> A | 7069 (9827, 4310) | 4.3                   | 83 (83, 82)        |
| MMY 19<br>(G <sub>ai2</sub> ) | Wild-type              | 2843 ± 1141       | 1                     | 91 ± 8             |
|                               | R103 <sup>3.50</sup> A | -                 | -                     | 2 (2, 1)           |
|                               | I107 <sup>3.54</sup> A | -                 | -                     | 1 (0, 1)           |
|                               | L213 <sup>IL3</sup> A  | 272 (199, 345)    | 0.1                   | 100 (100, 99)      |
|                               | S235 <sup>6.36</sup> A | -                 | -                     | 19 (8, 31)         |
|                               | L236 <sup>6.37</sup> A | -                 | -                     | 50 (60, 40)        |
| MMY 20<br>(G <sub>ai3</sub> ) | Wild-type              | 384 ± 158         | 1                     | 99 ± 7             |
|                               | R103 <sup>3.50</sup> A | -                 | -                     | 6 (10, 2)          |
|                               | I107 <sup>3.54</sup> A | -                 | -                     | 3 (3, 3)           |
|                               | L213 <sup>IL3</sup> A  | 90 (42, 137)      | 0.2                   | 102 (107, 97)      |
|                               | S235 <sup>6.36</sup> A | 437 (501, 372)    | 1.1                   | 77 (75, 80)        |
|                               | L236 <sup>6.37</sup> A | 5375 (4700, 6050) | 14                    | 85 (87, 84)        |
| MMY 21<br>(G <sub>ai4</sub> ) | Wild-type              | 212 ± 91          | 1                     | 108 ± 7            |
|                               | R103 <sup>3.50</sup> A | -                 | -                     | 4 (5, 2)           |
|                               | I107 <sup>3.54</sup> A | -                 | -                     | 1 (0, 1)           |
|                               | L213 <sup>IL3</sup> A  | 34 (17, 51)       | 0.2                   | 107 (108, 106)     |
|                               | S235 <sup>6.36</sup> A | 664 (552, 776)    | 3.1                   | 80 (78, 82)        |
|                               | L236 <sup>6.37</sup> A | 1335 (783, 1887)  | 6.3                   | 99 (104, 94)       |
| MMY 23<br>(G <sub>ai1</sub> ) | Wild-type              | 305 ± 137         | 1                     | 91 ± 8             |
|                               | R103 <sup>3.50</sup> A | -                 | -                     | 9 (15, 3)          |
|                               | I107 <sup>3.54</sup> A | 7629 (9162, 6095) | 25                    | 37 (38, 37)        |
|                               | L213 <sup>IL3</sup> A  | 108 (72, 143)     | 0.4                   | 95 (96, 94)        |
|                               | S235 <sup>6.36</sup> A | 84 (103, 65)      | 0.3                   | 82 (76, 88)        |
|                               | L236 <sup>6.37</sup> A | 411 (398, 424)    | 1.3                   | 98 (102, 95)       |
| MMY 24<br>(G <sub>ai3</sub> ) | Wild-type              | 59 ± 10           | 1                     | 113 ± 5            |
|                               | R103 <sup>3.50</sup> A | -                 | -                     | 9 (7, 10)          |
|                               | I107 <sup>3.54</sup> A | -                 | -                     | 2 (2, 1)           |
|                               | L213 <sup>IL3</sup> A  | 49 (25, 72)       | 0.8                   | 104 (113, 96)      |
|                               | S235 <sup>6.36</sup> A | 175 (174, 176)    | 3                     | 105 (109, 102)     |
|                               | L236 <sup>6.37</sup> A | 680 (504, 855)    | 11.6                  | 112 (121, 103)     |
| MMY 28<br>(G <sub>as</sub> )  | Wild-type              | 25 ± 6            | 1                     | 112 ± 4            |
|                               | R103 <sup>3.50</sup> A | 57 (53, 61)       | 2.2                   | 95 (98, 92)        |
|                               | I107 <sup>3.54</sup> A | 47 (25, 69)       | 1.9                   | 103 (100, 106)     |
|                               | L213 <sup>IL3</sup> A  | 23 (31, 15)       | 0.9                   | 105 (104, 106)     |
|                               | S235 <sup>6.36</sup> A | 33 (42, 24)       | 1.3                   | 105 (110, 100)     |
|                               | L236 <sup>6.37</sup> A | 538 (755, 321)    | 21                    | 96 (95, 98)        |

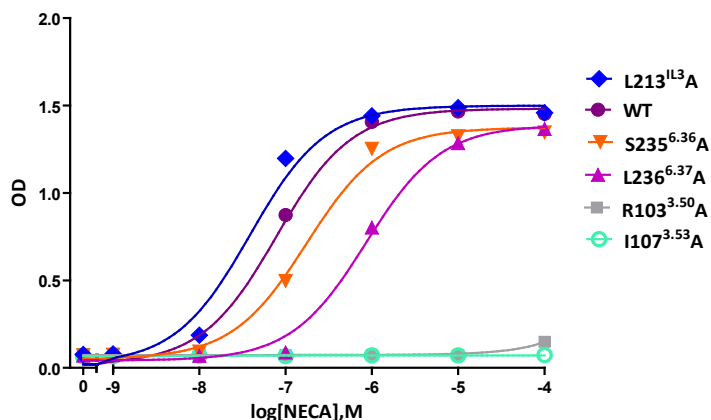


**Fig. 3** Concentration-effect curves from liquid assay experiments. Curves are shown of the wild-type, and five mutant receptors L213<sup>IL3</sup>A, S235<sup>6.36</sup>A, L236<sup>6.37</sup>A, R103<sup>3.50</sup>A and I107<sup>3.53</sup>A in the MMY24(G<sub>α13</sub>) strain responding to the adenosine receptor agonist NECA. The assay was performed in YNB-ULH medium.

### Determination of expression level of the hA<sub>2B</sub>R in different yeast strains

In Figure 4A a Western blot analysis of the expression levels of the WT hA<sub>2B</sub>R and three mutants is shown. In each gel the antibody used recognized the top and bottom bands as specific bands of the hA<sub>2B</sub>R while the middle one was used as a reference band, since it is not specific for the receptor as evidenced by the MMY12 strain carrying the plasmid pDT-PGK without receptor. Quantitative bar graphs derived from the data in Figure 4A are shown in Figure 4B. Expression levels of the wild-type receptor in most strains were quite comparable (Fig. 4B). Even though mutants R103A and I107 did not respond to NECA in the liquid assay experiments, they did express in all yeast strains, except for MMY21\_I107A (Fig. 4B). These data confirm that the transformation protocols used led to robust receptor expression in (almost) all cases and, hence, provide further proof of the validity of the activation profiles established. Moreover, it seems a certain degree of receptor expression is sufficient for receptor activation. As an example, the density of the L213<sup>IL3</sup>A mutant was lowest in MMY24 and highest in MMY28. Nevertheless, EC<sub>50</sub> and E<sub>max</sub> values for NECA were the virtually the same in both strains. To save costly (and commercially unavailable) antibody we did not screen S235A and L236A mutant receptors, since their transferred strains always showed NECA concentration-response curves with high E<sub>max</sub> values.

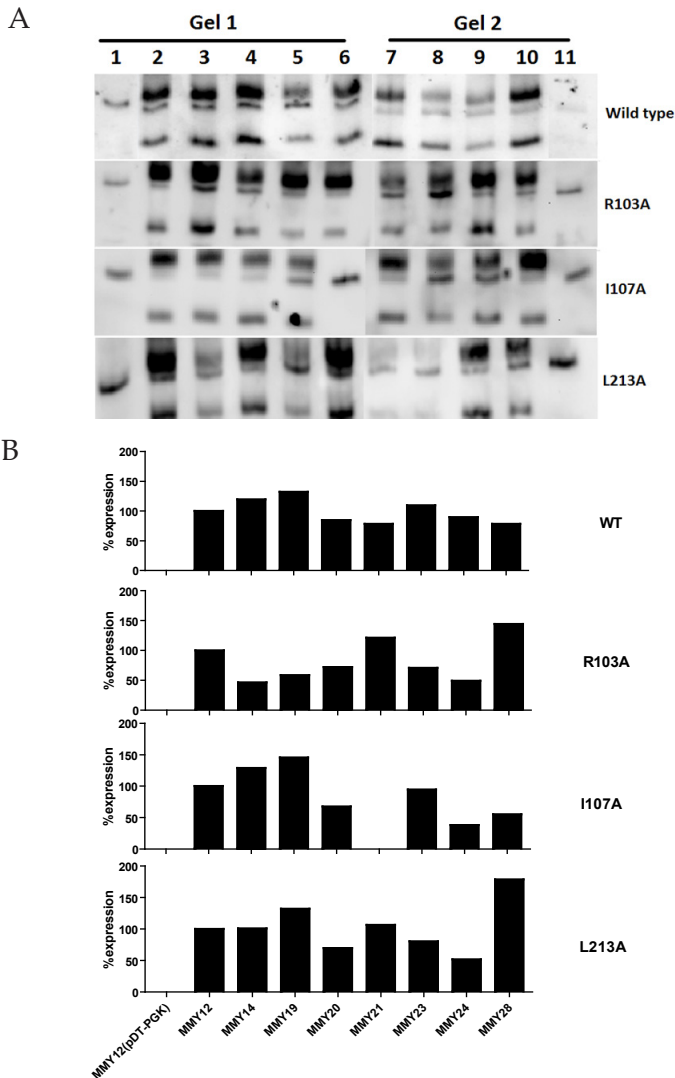


**Fig. 4** Western blot analysis of the wild-type hA<sub>2B</sub>R and R103A, I107A and L213A mutations from top to bottom panel as expressed in different MMY strains. (A) Gel 1: Lane 1, MMY12 carrying pDT-PGK without receptor; Lane 2- 6, MMY12, MMY14, MMY19, MMY20 and MMY21 carrying pDT-PGK\_A<sub>2B</sub> wild-type or mutant receptor. Gel 2: Lane7-10, MMY23, MMY24, MMY28 and MMY12 carrying pDT-PGK\_A<sub>2B</sub> mutant receptor; Lane 11, MMY12 carrying pDT-PGK without receptor. The A<sub>2B</sub> receptor specific bands are 29 kDa and 50 kDa, which are absent in MMY12 carrying pDT-PGK without receptor; Nonspecific band at approx. 45 kDa was used as loading control, which also appeared in MMY12 carrying pDT-PGK without receptor. (B) Bar graphs were calculated from a densitometric analysis of the blots. The ratio was determined between the density of the specific bands and that of the nonspecific band that is always present on the blots. MMY12 carrying wild-type or mutant receptor was set as 100% and MMY12 carrying the empty vector pDT-PGK without receptor was set as 0%.

## Ligand binding assay of wild-type and mutant hA<sub>2B</sub>R expressed in MMY24(G<sub>ai3</sub>)

To investigate whether the binding affinity of NECA was changed in the mutated receptors, we performed a number of radioligand binding experiments. Traditionally, this assay is cumbersome in yeast cells, but we managed to obtain sufficient levels of specific [<sup>3</sup>H]PSB-603 binding to do displacement assays on wild-type, L213A and L236A receptors. The two mutant receptors had a similar IC<sub>50</sub> value for NECA displacing [<sup>3</sup>H]PSB-603 binding compared to the wild-type receptor (Table 3). However, the binding affinity of the radiolabeled antagonist for the other mutants, R103A, I107A and S235A, appeared to be decreased. As a consequence we did not obtain a high enough window of specific [<sup>3</sup>H]PSB-603 binding to perform a radioligand displacement assay.

**Table 3.** Radioligand binding experiments of wild-type and mutant hA<sub>2B</sub>R receptors expressed in MMY24(G<sub>ai3</sub>) using 1.5 nM [<sup>3</sup>H]PSB-603. Specific binding of wild-type receptor was set at 100%. IC<sub>50</sub> values were obtained from competition binding curves of five independent experiments, performed in duplicate.

| Mutant    | % specific binding | IC <sub>50</sub> ( $\mu$ M) |
|-----------|--------------------|-----------------------------|
| Wild-type | 100                | 1.85 $\pm$ 0.87             |
| R103A     | 0                  | nd                          |
| I107A     | 12                 | nd                          |
| L213A     | 94                 | 1.90 $\pm$ 1.64             |
| S235A     | 20                 | nd                          |
| L236A     | 158                | 1.88 $\pm$ 0.6              |

nd: not determined

## Discussion

Even though the mechanisms of interaction between GPCRs and their G proteins are largely unknown, the  $\alpha$ 4-helix and  $\alpha$ 4- $\beta$ 6 loop<sup>[34, 35]</sup>, the N-terminus<sup>[36]</sup> and C-terminus of G <sub>$\alpha$</sub>  subunits<sup>[37]</sup> have been described to be important for GPCR-G <sub>$\alpha$</sub>  protein binding and selectivity. Of those the C-terminus of the G <sub>$\alpha$</sub>  subunit appears most intimately involved in binding the receptor. This was already evident from available crystal structures<sup>[23, 30]</sup> and further confirmed in molecular dynamics

calculations by Kling et al., to show that three residues at the C-terminus of G<sub>αs</sub> are in close contact with at least 5 amino acids of the β<sub>2</sub>AR<sup>[38]</sup>. In the present study, we examined the mechanism of interaction between the A<sub>2B</sub> receptor and the last five amino acid residues in the C-terminus of G<sub>α</sub> subunits using a functional yeast system combined with homology modeling and mutagenesis experiments.

### **G protein-coupling profiles of the wild-type A<sub>2B</sub> receptor**

We found that the wild-type hA<sub>2B</sub>R can activate many humanized G protein pathways, which is consistent with earlier findings by Brown et al. that the hA<sub>2B</sub>R is quite promiscuous as it recognizes most strains with a similar rank order of activation<sup>[19]</sup>. These strains possess different humanized G proteins, in which the last five amino acid residues of the endogenous Gpa1p C-terminal have been replaced with the same sequence from mammalian G<sub>α</sub> proteins, covering the four major classes: G<sub>αi</sub>, G<sub>αs</sub>, G<sub>αq</sub> and G<sub>α12</sub>. It is worth noting that the differences in activation profiles found in the present study can only be due to the variation in the five terminal amino acids of the humanized C-terminus of the G<sub>α</sub> subunit. This has the advantage of providing a detailed snapshot of G protein activation without confounding factors such as further differences in the composition of the various G<sub>α</sub> subunits.

The A<sub>2B</sub> receptor is preferentially coupled to the G<sub>s</sub> pathway and to a lesser degree to the G<sub>q</sub> pathway in many cells<sup>[39]</sup>, and these two G proteins also couple well in our yeast system (*S. cerevisiae* strains MMY28(G<sub>αs</sub>), MMY14(G<sub>αq</sub>) and MMY21(G<sub>α14/q</sub>), respectively). Interestingly, the receptor appears to couple well to two strains with a G<sub>αi</sub> protein, MMY24(G<sub>αi3</sub>) and MMY23(G<sub>αi1</sub>), too, providing proof of the promiscuity mentioned above. However, this is not a “general” GPCR feature. For instance, Stewart et al used the same yeast system to study functional selectivity of agonists and antagonists of the adenosine A<sub>1</sub> receptor and learned that only the G<sub>i/o</sub> pathway was addressed<sup>[18]</sup>. Likewise, the hydroxy-carboxylic acid receptor HCA<sub>3</sub> can only activate the G<sub>i</sub> pathway through its agonist acifran (preliminary data not shown).

## G protein-coupling profiles of mutants of the hA<sub>2B</sub>R

In the present study we sought to identify amino acid residues on the hA<sub>2B</sub>R that are vital in G protein coupling. The  $\beta_2$ AR-G<sub>s</sub> crystal structure (PDB: 3SN6) was chosen as the template to predict such amino acids in the hA<sub>2B</sub>R. R103<sup>3.50</sup>, I107<sup>3.54</sup>, L213<sup>IL3</sup>, S235<sup>6.36</sup> and L236<sup>6.37</sup> were selected to be mutated into alanine because they are interacting with the last five amino acids of the G<sub>as</sub> protein in the  $\beta_2$ AR-G<sub>s</sub> crystal structure. We will discuss these five amino acids in the light of our findings.

### *Residues R103<sup>3.50</sup> and I107<sup>3.54</sup>*

These two residues (R103<sup>3.50</sup> and I107<sup>3.54</sup>) are located on the intracellular side of TM3 and are included in the consensus sequence (I/L)XXDR<sup>3.50</sup>YXX(I/V)<sup>3.54</sup>[32]. R<sup>3.50</sup> is a part of the most conserved motif in the class A GPCRs: Asp-Arg-Tyr (DRY). This arginine is 100% conserved within the subfamily of adenosine receptors and nucleotide-like receptors, and 97% of all Class A rhodopsin-like receptors. This is less so for I<sup>3.54</sup> with 54% overall conservation (Table 4).

Not surprisingly R<sup>3.50</sup> has been the subject of many mutation studies, exemplified by their high occurrence in the GPCRDB mutation database<sup>[40]</sup>. The DRY-motif is part of a so-called “ionic lock”<sup>[41, 42]</sup>, consisting of a number of interactions between the DRY-motif and amino acids in TM6; the interaction that is most prominent is the interaction between R<sup>3.50</sup> and a negatively charged residue in TM6, Asp (D) or Glu (E). These interactions are thought to stabilize the receptor in an inactive conformation and thereby decrease its basal activity<sup>[43]</sup>. When the receptor is activated the ionic lock is broken and TM6 is moving outward. Breaking the ionic lock through mutation might thus lead to constitutive activity, which was shown to be the case on the adenosine A<sub>3</sub> receptor<sup>[44]</sup>. While this mechanism seems to hold true for some receptors it does not hold for every GPCR, as on the histamine H<sub>4</sub> receptor<sup>[45]</sup>. R<sup>3.50</sup> in this case turned out to be very important for G protein coupling. Our own results comply with data found for the  $\alpha_{1b}$ -adrenergic receptor where mutations of R<sup>3.50</sup> resulted in a complete loss of receptor-mediated response in the majority of mutant receptors<sup>[46]</sup>.

It has been proposed that there are many other conserved residues that help R<sup>3.50</sup> switch the receptor on or off, such as D<sup>3.49</sup> and I/V<sup>3.54</sup>[32]. The latter position (3.54) is always conserved with a bulky  $\beta$ -branched, hydrophobic residue (Val or Ile). A mutagenesis study in the gonadotropin-releasing hormone (GnRH) receptor offered a hypothesis as to why there is a lack of receptor signaling in a receptor with a mutated I<sup>3.54</sup>. According to Ballesteros et al. I<sup>3.46</sup>, A<sup>3.49</sup>, and I<sup>3.54</sup>, all highly conserved amino acids, form a layer around R<sup>3.50</sup>, the so-called arginine-cage motif. I<sup>3.54</sup>A mutations caused significant reductions in receptor signaling efficacy and reduced the affinity for GnRH as well. In the WT receptor the bulky side chain of I<sup>3.54</sup> cannot move much as it readily clashes with the side chain of R<sup>3.50</sup>. This does not occur in the I<sup>3.54</sup>A mutant, which allows R<sup>3.50</sup> to take an unfavorable conformation with an orientation to the aqueous cytoplasm. This might prevent R<sup>3.50</sup> from taking part in receptor activation. Thus the purpose of I<sup>3.54</sup> appears to be a defined and strictly controlled positioning of R<sup>3.50</sup>[32].

The results from our yeast screening assay add a layer of detail to these general findings, in that some G proteins seem more affected than others. We found that mutation to alanine of R103<sup>3.50</sup> and I107<sup>3.54</sup> in the hA<sub>2B</sub>R abolished many humanized G protein pathways (Table 2) and, hence, we concluded they are very important for interaction with humanized G proteins. R103<sup>3.50</sup> is crucial for each pathway, except for G<sub>as</sub>, whereas I107<sup>3.54</sup> is vital for most G protein pathways as well, although after mutation some interaction remained with both G<sub>ai1</sub> and G<sub>as</sub>.

**Table 4.** Sequence conservation of the four helical amino acids involved in G protein interaction, among adenosine receptors, nucleotide-like receptors\*, and class A rhodopsin-like receptors as found on GMOS (GPCRs Motif Searcher, <http://lmc.uab.cat/gmos/>).

| Amino acid in A <sub>2B</sub> | Conservation in Adenosine receptors | Most occurring | Conservation in Nucleotide-like receptors | Most occurring | Conservation in Class A rhodopsin-like receptors | Most occurring |
|-------------------------------|-------------------------------------|----------------|---|----------------|--|----------------|
| R103 <sup>3.50</sup>          | 100.0%                              | R - 100%       | 100.0%                                    | R - 100%       | 96.98%   | R - 96.98%     |
| I107 <sup>3.54</sup>          | 35.29%                              | V - 64.70%     | 41.74%                                    | V - 46.60%     | 53.68%   | I - 53.68%     |
| S235 <sup>6.36</sup>          | 85.29%                              | S - 85.29%     | 33.00%                                    | S - 33.00%     | 2.81%  | T - 32.25%     |
| L236 <sup>6.37</sup>          | 85.29%                              | L - 85.29%     | 36.89%                                    | L - 36.89%     | 38.59%   | L - 38.59%     |

\* Nucleotide-like receptors: adenosine A<sub>1</sub>, A<sub>2A</sub>, A<sub>2B</sub>, A<sub>3</sub> receptors; P2RY1, 4, 5, 6, 8, 9, 10, 11; GPR23, 35, 91, 92, 174.

### *Other three residues L213<sup>IL3</sup>, S235<sup>6.36</sup> and L236<sup>6.37</sup>*

Even though the investigated mutants only have one residue altered at the time, they show substantial differences in ligand activation of the receptor. A prominent enhancement was seen with the L213<sup>IL3</sup>A mutant; in all cases/strains NECA was more active than on the wild-type receptor, particularly in MMY19(G<sub>α12</sub>), with a 10-fold increase in potency. This result shows once more the dependency of agonist potency on amino acids other than those in the ligand binding site, and may even shed light on pharmacological principles such as receptor reserve. Apparently, the leucine on position 213 in the wild-type receptor acts as a deactivating switch.

The role of S<sup>3.36</sup> seems to be somewhat more ambiguous. This residue when mutated to alanine caused mostly a decrease of receptor signaling. S<sup>6.36</sup> is much conserved (Table 4) within the adenosine receptor subfamily (85%), but less so in the nucleotide-like receptors (33%) and hardly in all class A rhodopsin-like receptors (2.8%). Several mutations have been made in different receptors on the 6.36 position but none of the original amino acids was a serine. The closest mutation is a T<sup>6.36</sup>A in the human muscarinic acetylcholine M1 receptor where the mutant did not significantly differ from wild-type in PI turnover<sup>[47]</sup>. In the present study, the S2<sup>6.36</sup>A mutation showed a most divergent G protein profile: improved activation efficiency in MMY28(G<sub>αs</sub>) and MMY23(G<sub>αi1</sub>); no change in

MMY20(G<sub>α13</sub>) similar to MMY12(G<sub>αWT</sub>); decreased activation in MMY14(G<sub>αq</sub>), MMY24(G<sub>αi3</sub>), MMY21(G<sub>α14</sub>) and a complete loss of activation in MMY19(G<sub>α12</sub>) (Table 2). Apparently the change from a hydrophilic (serine) to a hydrophobic (alanine) amino acid is dealt with differently by the G proteins studied.

L<sup>6.37</sup> is quite conserved: 85% in adenosine receptors, 37% in nucleotide-like receptors, and 39% in all class A rhodopsin-like receptors. In the A<sub>2A</sub> receptor the L<sup>6.37</sup>A mutation along with several others was used to provide receptor thermostabilization for crystallographic purposes<sup>[48]</sup>. The mutant caused no effect on ligand pharmacology. In our hands, the L236<sup>6.37</sup>A mutation decreased activation in all humanized G protein pathways, most outspoken for MMY28. Apparently, the leucine residue is vital for G protein interaction and activation.

### Function of hydroxyl-group at C-terminus of G<sub>α</sub> subunits for wild-type hA<sub>2B</sub>R

The slight differences in amino acid composition in some of the G<sub>α</sub> subunits allow an almost atomic dissection of the observed effects. There is an 8-fold potency difference of NECA in the two G<sub>q</sub> pathway strains MMY21(G<sub>α14</sub>) with an EC<sub>50</sub> value of 212 nM and MMY14(G<sub>αq</sub>) with an EC<sub>50</sub> value of 1641 nM. Both have the same amino acid residues at the C-terminus of the G<sub>α</sub> protein except for the fourth residue position counting from the end of the C-terminus with a tyrosine in MMY14 and a phenylalanine in MMY21 (Table 1). The only difference between tyrosine and phenylalanine is a hydroxyl-group, which leads to the large decrease in potency for NECA. However, there is an opposite phenomenon at the last amino acid of the C-terminus between two G<sub>ai</sub> pathway strains, MMY24(G<sub>αi3</sub>) and MMY23(G<sub>αi1</sub>). A tyrosine as last amino acid of the end of the C-terminus position of MMY24 yielded an EC<sub>50</sub> value of 59 nM for NECA, whereas the phenylalanine on the same position in MMY23 gave an EC<sub>50</sub> value of 305 nM (Tables 1 and 2). This particular tyrosine hydroxyl-group is apparently enough to decrease the EC<sub>50</sub> value by 6-fold, which is equivalent to an increase of activation and NECA potency. Taken together, subtle changes such as the presence or absence of a hydroxyl-group located in the C-terminus of the G<sub>α</sub> protein control activation of GPCRs.

## Concluding remarks

We reported on a yeast system that is very well suited for the study of a G protein-coupled receptor (the hA<sub>2B</sub>R in this case), its activation and its G protein preference. This highly efficient and inexpensive screening system was used to map residues at the cytoplasmic side of the receptor and in the C-terminus of different G<sub>α</sub> subunits important for receptor activation. The results provided detailed information about receptor/G protein binding and G protein selectivity.

## Acknowledgements

Rongfang Liu thanks the China Scholarship Council (CSC) for her PhD scholarship. NWO provided a TOP grant to A.P. IJ. (714.011.001). The authors are grateful to Prof C.E. Müller of Bonn University for the generous gift of [<sup>3</sup>H] PSB-603 and to Simon Dowell from GSK for providing the yeast strains and experimental protocols.

## References

- [1] Oldham, W.M., et al. *Mechanism of the receptor-catalyzed activation of heterotrimeric G proteins*. Nat. Struct. Mol. Biol. (2006) 13: 772-777.
- [2] Baltoumas, F.A., et al. *Interactions of the alpha-subunits of heterotrimeric G-proteins with GPCRs, effectors and RGS proteins: A critical review and analysis of interacting surfaces, conformational shifts, structural diversity and electrostatic potentials*. J. Struct. Biol. (2013) 182: 209-218.
- [3] Fredholm, B.B., et al. *Structure and function of adenosine receptors and their genes*. Naunyn-Schmiedeberg's Arch. Pharmacol. (2000) 362: 364-374.
- [4] Fredholm, B.B., et al. *Comparison of the potency of adenosine as an agonist at human adenosine receptors expressed in Chinese hamster ovary cells*. Biochem. Pharmacol. (2001) 61: 443-448.
- [5] Wei, W., et al. *Blocking A<sub>2B</sub> adenosine receptor alleviates pathogenesis of experimental autoimmune encephalomyelitis via inhibition of IL-6 production and Th17 differentiation*. J. Immunol. (2013) 190: 138-146.
- [6] Wei, Q., et al. *A<sub>2B</sub> adenosine receptor blockade inhibits growth of prostate cancer cells*. Purinergic Signal. (2013) 1-10.
- [7] Stagg, J., et al. *Anti-CD73 antibody therapy inhibits breast tumor growth and metastasis*.

- Proc. Natl. Acad. Sci. (2010) 107: 1547-1552.
- [8] Owen, S.J., et al. *Loss of adenosine A<sub>2B</sub> receptor mediated relaxant responses in the aged female rat bladder; effects of dietary phytoestrogens.* Naunyn-Schmiedeberg's Arch. Pharmacol. (2012) 385: 539-549.
- [9] Cekic, C., et al. *Adenosine A<sub>2B</sub> receptor blockade slows growth of bladder and breast tumors.* J. Immunol. (2012) 188: 198-205.
- [10] Koscsó, B., et al. *Stimulation of A<sub>2B</sub> adenosine receptors protects against trauma-hemorrhagic shock-induced lung injury.* Purinergic Signal. (2013) 1-6.
- [11] Bot, I., et al. *Adenosine A<sub>2B</sub> receptor agonism inhibits neointimal lesion development after arterial injury in apolipoprotein E-deficient mice.* Arterioscler. Thromb. Vasc. Biol. (2012) 32: 2197-2205.
- [12] Pausch, M.H. *G-protein-coupled receptors in Saccharomyces cerevisiae: high-throughput screening assays for drug discovery.* Trends Biotechnol. (1997) 15: 487-494.
- [13] Peeters, M.C., et al. *Three "hotspots" important for adenosine A<sub>2B</sub> receptor activation: a mutational analysis of transmembrane domains 4 and 5 and the second extracellular loop.* Purinergic Signal. (2011) 1-16.
- [14] Mathew, E., et al. *Functional fusions of T4 lysozyme in the third intracellular loop of a G protein-coupled receptor identified by a random screening approach in yeast.* Protein Eng. Des. Sel. (2013) 26: 59-71.
- [15] Jaeschke, H., et al. *Preferences of transmembrane helices for cooperative amplification of G<sub>as</sub> and G<sub>aq</sub> signaling of the thyrotropin receptor.* Cell. Mol. Life Sci. (2008) 65: 4028-4038.
- [16] Evans, B.J., et al. *Expression of CXCR4, a G-protein-coupled receptor for CXCL12 in Yeast: identification of new-generation inverse agonists.* Methods Enzymol. (2009) 460: 399-412.
- [17] Minic, J., et al. *Yeast system as a screening tool for pharmacological assessment of G protein coupled receptors.* Curr. Med. Chem. (2005) 12: 961-969.
- [18] Stewart, G.D., et al. *Determination of adenosine A<sub>1</sub> receptor agonist and antagonist pharmacology using Saccharomyces cerevisiae: implications for ligand screening and functional selectivity.* J. Pharm. Exp. Ther. (2009) 331: 277-286.
- [19] Brown, A.J., et al. *Functional coupling of mammalian receptors to the yeast mating pathway using novel yeast/mammalian G protein  $\alpha$  subunit chimeras.* Yeast (2000) 16: 11-22.
- [20] Dowell, S.J. and Brown, A.J. *Yeast assays for G protein-coupled receptors.* Methods Mol. Biol. (2009) 552: 213-229.
- [21] Dowell, S.J. *Yeast assays for G-protein-coupled receptors.* Receptors Channels (2002) 8: 343-352.
- [22] Cardozo, T., et al. *Homology modeling by the ICM method.* Proteins: Struct., Funct., Bioinf. (2004) 23: 403-414.
- [23] Rasmussen, S.G., et al. *Crystal structure of the  $\beta_2$  adrenergic receptor-G<sub>s</sub> protein complex.* Nature (2011) 477: 549-555.
- [24] DeLano, D.W., *The PyMOL Molecular Graphics System, Version 1.5. 0.4 Schrödinger, LLC.*
- [25] Gietz, D., et al. *Improved method for high efficiency transformation of intact yeast cells.*

- Nucleic Acids Res. (1992) 20: 1425.
- [26] Li, Q., et al. ZM241385, DPCPX, MRS1706 are inverse agonists with different relative intrinsic efficacies on constitutively active mutants of the human adenosine A<sub>2B</sub> receptor. *J. Pharmacol. Exp. Ther.* (2007) 320: 637-645.
- [27] Feoktistov, I., et al. Immunological characterization of A<sub>2B</sub> adenosine receptors in human mast cells. *Drug Dev. Res.* (2003) 58: 461-471.
- [28] Peeters, M., et al. The role of the second and third extracellular loops of the adenosine A<sub>1</sub> receptor in activation and allosteric modulation. *Biochem. Pharmacol.* (2012) 84: 76-87.
- [29] Venkatakrisnan, A., et al. Molecular signatures of G-protein-coupled receptors. *Nature* (2013) 494: 185-194.
- [30] Scheerer, P., et al. Crystal structure of opsin in its G-protein-interacting conformation. *Nature* (2008) 455: 497-502.
- [31] Fredholm, B.B., et al. International union of basic and clinical pharmacology. LXXXI. nomenclature and classification of adenosine receptors an update. *Pharmacol. Rev.* (2011) 63: 1-34.
- [32] Ballesteros, J., et al. Functional microdomains in G-protein-coupled receptors the conserved arginine-cage motif in the gonadotropin-releasing hormone receptor. *J. Biol. Chem.* (1998) 273: 10445-10453.
- [33] Ballesteros, J.A. and Weinstein, H. Integrated methods for the construction of three-dimensional models and computational probing of structure-function relations in G protein-coupled receptors. *Methods Neurosci.* (1995) 25: 366-428.
- [34] Bae, H., et al. Two amino acids within the  $\alpha 4$  helix of G<sub>ait</sub> mediate coupling with 5-hydroxytryptamine 1B receptors. *J. Biol. Chem.* (1999) 274: 14963-14971.
- [35] Bae, H., et al. Molecular determinants of selectivity in 5-hydroxytryptamine 1B receptor-G protein interactions. *J. Biol. Chem.* (1997) 272: 32071-32077.
- [36] Taylor, J.M., et al. Binding of an alpha 2 adrenergic receptor third intracellular loop peptide to G beta and the amino terminus of G alpha. *J. Biol. Chem.* (1994) 269: 27618-27624.
- [37] Blahos, J., et al. Extreme C terminus of G protein  $\alpha$ -subunits contains a site that discriminates between G<sub>i</sub>-coupled metabotropic glutamate receptors. *J. Biol. Chem.* (1998) 273: 25765-25769.
- [38] Kling, R.C., et al. Active-state models of ternary GPCR complexes: determinants of selective receptor-G-protein coupling. *PLOS ONE* (2013) 8: e67244.
- [39] Thimm, D., et al. Ligand-specific binding and activation of the human adenosine A<sub>2B</sub> receptor. *Biochemistry* (2013) 52: 726-740.
- [40] Vroiling, B., et al. GPCRDB: information system for G protein-coupled receptors. *Nucleic Acids Res.* (2011) 39: D309-D319.
- [41] Vogel, R., et al. Functional role of the "ionic lock"—an interhelical hydrogen-bond network in family A heptahelical receptors. *J. Mol. Biol.* (2008) 380: 648-655.
- [42] Scheer, A., et al. Constitutively active mutants of the alpha 1B-adrenergic receptor: role of highly conserved polar amino acids in receptor activation. *EMBO J.* (1996) 15: 3566.
- [43] Flanagan, C.A. A GPCR that is not "DRY". *Mol. Pharmacol.* (2005) 68: 1-3.

- [44] Chen, A., et al. *Constitutive activation of A<sub>3</sub> adenosine receptors by site-directed mutagenesis*. *Biochem. Biophys. Res. Commun.* (2001) 284: 596-601.
- [45] Schneider, E.H., et al. *Impact of the DRY motif and the missing "ionic lock" on constitutive activity and G-protein coupling of the human histamine H4 receptor*. *J. Pharmacol. Exp. Ther.* (2010) 333: 382-392.
- [46] Scheer, A., et al. *Mutational analysis of the highly conserved arginine within the Glu/Asp-Arg-Tyr motif of the  $\alpha$ 1b-adrenergic receptor: effects on receptor isomerization and activation*. *Mol. Pharmacol.* (2000) 57: 219-231.
- [47] Högger, P., et al. *Activating and inactivating mutations in N- and C-terminal i3 loop junctions of muscarinic acetylcholine Hm1 receptors*. *J. Biol. Chem.* (1995) 270: 7405-7410.
- [48] Doré, A.S., et al. *Structure of the adenosine A<sub>2A</sub> receptor in complex with ZM241385 and the Xanthines XAC and Caffeine*. *Structure* (2011) 19: 1283-1293.
- [49] Simon, M.I., et al. *Diversity of G proteins in signal transduction*. *Science* (1991) 252: 802-808.

